inately single-bond character and the S(1)–N(1) and S(1)–N(4) bonds with distances of 1.533 (3) and 1.537 (3) Å double bond character. These distances are similar to those of 1.702 (3) and 1.536 (3) Å for the formally single and double S–N bonds in the –N=S=N– handle of S_5N_6.[5] Perhaps the best way of regarding the structure of the S_4N_5 unit in **6** is, therefore, as an S_3N_3 ring with a high degree of π delocalization bridged by an –N=S=N– unit between S(2) and S(4). This description is not surprising as the three sulfur atoms in the S_3N_3 ring all display the coordination number 3, that in the –N=S=N– handle displays only 2. Raising the coordination number of sulfur leads to a contraction of its orbitals allowing thereby a better overlap with nitrogen orbitals, which leads to an increase in S–N bond strength. The S_3N_3 ring containing S(2), S(3), and S(4) is in a chair conformation with S(3) and N(5) displaced –0.365 and 0.616 Å from the least-squares plane through the remaining four atoms (distances: N(3), –0.009; S(4), 0.009; S(2), –0.009; N(2), 0.009 Å). In contrast the second S_3N_3 ring containing S(1), S(2), and S(4) displays a basically envelope conformation with N(5) as the flap. The distances from the least-squares plane through N(1), S(2), S(4), and N(4) are as follows: S(1), –0.112; N(1), 0.017; S(2), –0.017; N(5), –0.765; S(4), 0.017; N(4), –0.017 Å. Whereas the anions $S_4N_5^-$ and $S_4N_5O^-$ display six S···S separations of length respectively 2.71–2.75 and 2.63–2.74 Å, only five such interactions in the range 2.78–2.81 Å are to be observed for $S_4N_5^+$. The sixth pair of sulfur atoms S(1) and S(3) are at 4.01 Å from another. A similar state of affairs is observed in **6** where five S···S interactions are found in the range 2.736–2.846 Å with the sixth distance S(1)···S(3) = 3.814 (1) Å. This distance is presumably longer in $S_4N_5^+$ as a result of some preferential delocalization of cation charge on the sulfur atoms S(1) and S(3) in this moiety.[3]

The striking difference in the N–S distances to S(6) in the side chain of **6** correlates with the observation that the bond angle at N(7) is 20.2° wider than at N(5). Similar short N–S distances of 1.507 and 1.498 Å have been observed for this bond in the derivatives $(CH_3)_2Si_2N_6S_3$[14] and $(CH_3)_4Si_2N_4S_2$[15] when the nitrogen is at the same time bonded to silicon. This may be caused by a change in the electron density of the σ skeleton, an effect which is known for silicon.[16] The N–Si distance of 1.725 (2) Å lies in typical range for this bond.[17]

Acknowledgment. The authors are grateful to the Deutsche Forschungsgemeinschaft and the Fonds der Chemischen Industrie for financial support of this work. M.N.S.R. thanks the Alexander von Humboldt-Foundation for the award of a fellowship.

Registry No. **1**, 71699-97-3; **2**, 18156-25-7; **3**, 68993-02-2; **4**, 19923-46-7; **5**, 71901-54-7; **6**, 71901-55-8; $N[Sn(CH_3)_3]_3$, 1068-70-8.

Supplementary Material Available: Compilations of observed and calculated structure factors on an absolute scale (22 pages). Ordering information is given on any current masthead page.

(14) B. Krebs, unpublished results.
(15) H. W. Roesky and H. Wiezer, *Chem.-Ztg.*, **97**, 661 (1973); G. Ertl and J. Weiss, *Z. Naturforsch., B*, **29**, 803 (1974); H. W. Roesky and H. Wiezer, *Angew. Chem., Int. Ed. Engl.*, **13**, 146 (1974).
(16) H. Bock and W. Ensslin, *Angew. Chem., Int. Ed. Engl.*, **10**, 404 (1971).
(17) H. W. Roesky, *Z. Naturforsch., B*, **31**, 680 (1976).

Contribution from the Department of Chemistry, Rutgers University, New Brunswick, New Jersey 08903, Department of Chemistry, Rutgers University, Newark, New Jersey 07102, and the School of Chemical Sciences, University of Illinois, Urbana, Illinois 61801

Crystal Structure and Magnetic Properties of the Cluster Complex $Cu^I_8Cu^{II}_6[SC(CH_3)_2CH_2NH_2]_{12}Cl\cdot 3.5SO_4\cdot\sim 20H_2O$, a Mixed-Valence Copper–Mercaptide Species

HARVEY J. SCHUGAR,*[1a] CHIA-CHIH OU,[1a] JOHN A. THICH,[1a] JOSEPH A. POTENZA,*[1a] TIMOTHY R. FELTHOUSE,[1b] MUIN S. HADDAD,[1b] DAVID N. HENDRICKSON,*[1b] WILLIAM FUREY, JR.,[1c] and ROGER A. LALANCETTE[1c]

Received June 7, 1979

The structure of the title complex (**1**) has been determined from three-dimensional X-ray data. $Cu^I_8Cu^{II}_6[SC(CH_3)_2CH_2NH_2]_{12}Cl\cdot 3.5SO_4\cdot\sim 20H_2O$ crystallizes in space group $C2/c$ (C_{2h}^6, No. 15) with $Z = 4$, $a = 18.318$ (3) Å, $b = 21.826$ (5) Å, $c = 28.829$ (6) Å, $\beta = 110.17$ (1)°, $d_{calcd} = 1.763$, and $d_{obsd} = 1.79$ (1) g/cm³. Least-squares refinement of 4790 reflections having $F^2 > 3\sigma(F^2)$ gave a conventional R factor of 0.10. The structure consists of discrete, centrosymmetric $Cu^I_8Cu^{II}_6[SC(CH_3)_2CH_2NH_2]_{12}Cl^{7+}$ clusters in which 14 copper ions are linked by 12 three-coordinate mercaptide ions and an eight-coordinate chloride ion. Each cluster contains a $Cu_{14}S_{12}Cl$ core similar to that reported for a related, anionic $Cu_{14}[SC(CH_3)_2CH(CO_2)NH_2]_{12}Cl^{5-}$ complex. The core consists of a distorted icosahedral arrangement of 12 sulfur atoms with 8 of the 20 triangular icosahedral faces occupied by cuprous ions which form an approximate cube (Cu(I)···Cu(I) = 3.264 (4)–3.341 (3) Å). The chloride ion is located at the common center of the cube and icosahedron. The remaining six core copper ions are cupric species which are located approximately along 6 of the 30 icosahedral edges to form a distorted octahedral array (Cu(II)···Cu(II) = 6.645 (4)–6.825 (4) Å). All core copper species are four-coordinate. The cupric species have approximately planar cis S_2N_2 ligand sets while the cuprous species show dominant triangular planar coordination geometry arising from S_3 ligation (Cu(I)–S = 2.268 (5)–2.297 (5) Å) with weakly bound apical chloride ions (Cu(I)–Cl = 2.852 (3)–2.880 (3) Å) oriented approximately normal to each triangular planar CuS_3 unit. Electronic spectral and magnetic properties of the title complex are presented and discussed. Effective magnetic moments of **1** fell in the range 1.79–2.50 μ_B at temperatures between 286 and 7.9 K; below 7.9 K, the magnetic moment decreased steadily to 2.37 μ_B at 4.2 K. Computer fits of the susceptibility data using the $\hat{H} = -2J\hat{S}_1\hat{S}_2$ spin–spin coupling model with $g = 2.066$ gave J values in the range 4.9–5.2 cm^{-1}. It is suggested that the observed ferromagnetic exchange interaction between Cu(II) ions is transmitted via S–Cu(I)–S superexchange pathways within the cluster. At both X- and Q-band frequencies and temperatures ranging from 300 to 9 K, EPR powder spectra of **1** consisted of a single derivative signal which we interpret as arising from electron exchange between Cu(II) ions at a frequency exceeding the difference between $g_{\parallel}$ and $g_{\perp}$ values. From an analysis of the electronic spectra of **1**, the intense purple color is attributed to $\sigma(S) \rightarrow Cu(II)$ charge transfer ($\epsilon \sim 3400$ per Cu(II)). Structural, magnetic, and electronic spectral data suggest that the cluster contains discrete Cu(I) and Cu(II) ions. We suggest that the Cu(II) ions in effect are ligated by the $Cu^I_8S_{12}Cl^{5-}$ substructure and its 12 aminoethyl "tails". Lastly, the synthesis and partial characterization of two yellow complexes which are oxidized by air to form **1** are described.

Introduction

Chemical studies of the copper–D-penicillamine ($HSC(CH_3)_2CHNH_3^+CO_2^-$) system may help illuminate the mechanism by which this drug mobilizes and promotes the urinary excretion of excess copper associated with Wilson's and other chronic liver diseases.[2] Patients undergoing oral

(1) (a) Rutgers, New Brunswick. (b) University of Illinois. (c) Rutgers, Newark.

(2) Birker, P. J. M. W. L.; Freeman, H. C. *J. Am. Chem. Soc.* **1977**, *99*, 6890–9.

0020-1669/80/1319-0543$01.00/0

penicillamine therapy are known to excrete both penicillamine disulfide and the mixed penicillamine–cysteine disulfide. The possibility that excreted copper is ligated by these disulfides prompted us to synthesize and characterize structurally the bis[copper(II) D-penicillamine disulfide] nonahydrate complex, a ligand-bridged dimeric species which exhibits high water solubility and an uncommon Cu^{II}–S(disulfide) bonding interaction.[3] A second species of biomedical interest is an intensely purple cluster complex noted originally by Sugiura and co-workers[4] and further characterized by several other groups.[5] We were unable to precipitate this cluster complex in a form suitable for a single-crystal X-ray diffraction study. However, we were able to crystallize a structurally similar copper cluster complex containing the decarboxylated penicillamine analogue $HSC(CH_3)_2CH_2NH_2$. A preliminary account of the structure and electronic spectra of this purple complex has been published.[6] We present here the complete structural details of this cluster complex along with its electronic spectra and magnetic properties over the temperature range 4.2–286 K. Also characterized in part are two yellow crystalline complexes which are oxidized by air to the purple cluster.

Experimental Section

1. Preparation of $Cu^{I}_8Cu^{II}_6[SC(CH_3)_2CH_2NH_2]_{12}Cl\cdot3.5SO_4\cdot\sim20H_2O$ (1). A stirred suspension of 1.6 g of CuO in 500 mL of H_2O containing 5.7 g of $ZnSO_4\cdot7H_2O$ and 5.6 g of $HSC(CH_3)_2CH_2NH_2\cdot HCl$[7] was heated to 75 °C over a 15-min period and then cooled to 25 °C. While being heated, the mixture became progressively more blue, and finally turned purple. Gray particulate matter (a mixture of fine black solid (CuO?) and yellow hexagonal plates) was collected by filtration. Additional yellow plates were deposited from the purple filtrate and are described below. After being stirred at 25 °C for 2 days in a loosely covered Erlenmeyer flask, a suspension of this gray solid in 400 mL of H_2O was converted into an intensely colored purple solution. Following the removal of a small quantity of fine blue solid by filtration, **1** was precipitated by the addition of 1 L of DMF to the filtrate. The crude product was purified by elution with H_2O (two times) from a Sephadex G-25 column. Partial evaporation (25 °C, 1 atm) of a H_2O/DMF solution of purified **1** yielded 2.5 g (61% based upon CuO) of gleaming black prisms.

Anal. Calcd for $Cu_{14}[SC(CH_3)_2CH_2NH_2]_{12}Cl\cdot3.5SO_4\cdot20H_2O$: Cu, 30.98; S, 17.31; N, 5.85; C, 20.08; H, 5.62; Cl, 1.23; S (as SO_4), 3.91; Zn, 0.0. Found: Cu, 31.35, 31.27, 31.88; S, 17.99, 17.80; N, 5.84, 6.05; C, 20.31, 21.08; H, 5.40, 5.31; Cl, 1.26, 1.28; S (as SO_4),[8] 4.31; Zn, 0 to "trace".

2. Preparation of Yellow Precursor (2). The yellow crystals that deposited from the *initial* purple filtrate were collected by filtration, washed with H_2O, 2-propanol, and acetone, and dried in air (yield 0.17 g). Examination of the crystals with a polarizing microscope indicated that the hexagonal face coincided with a threefold or higher crystallographic axis. By use of X-ray techniques, examination of 12 crystals, including a vanishingly thin hexagonal plate, demonstrated that each crystal was twinned. A density of 1.67 (1) g/cm^3 was observed for **2** by using a $CCl_4/C_2H_2Br_4$ gradient calibrated with standards. Examination of the product by infrared spectral techniques revealed the presence of SO_4 (strong absorptions at ~1110 and ~610 cm^{-1}) and the absence of –SH absorption in the 2500-cm^{-1} region. This, coupled with the absence of the strong characteristic absorptions of coordinated NH_2 in the 3200-cm^{-1} spectral region suggests that the ligand is $^-SC(CH_3)_2CH_2NH_3^+$. On the basis of the results obtained for complex **1** and a second yellow precursor, complex **3** (vide infra), complex **2** very likely is a high molecular weight cluster complex. The formulation shown below is merely a suggestion which is in fair agreement with the observed elemental analyses and spectral observations.

Anal. Calcd for $Cu_8[SC(CH_3)_2CH_2NH_3]_8\cdot4SO_4\cdot H_2O$: Cu, 28.14; N, 6.20; S, 21.30; C, 21.28; H, 5.35; Cl, 0.0. Found: Cu, 27.73; N, 6.31; S, 21.37; C, 22.43; H, 5.36; Cl, 0.31.

3. Preparation of a Second Yellow Precursor (3). By use of standard Schlenk techniques, a yellow solution of 0.28 g (2 mmol) of $HSC(CH_3)_2CH_2NH_2\cdot HCl$ and 0.66 g (2 mmol) of $Cu(CH_3CN)_4ClO_4$[9] in 130 mL of hot deoxygenated H_2O was prepared and filtered through a fine frit. A Schlenk tube containing the filtrate was placed in a Dewar containing hot H_2O and cooled to 25 °C over a period of approximately 1 day. A yellow crystalline product was separated from the colorless solution by filtration, washed with distilled H_2O, and dried in air. Examination of the yellow hexagonal plates with a polarizing microscope revealed that the six sides displayed sharp extinctions, whereas the hexagonal faces were totally extinct for all rotations of the crystal. A density of 1.99 (1) g/cm^3 was determined for **3** by use of a CCl_4/CH_2Br_2 gradient calibrated with standards. The presence of Cl^- in **3** was confirmed with Ag^+ after the mercaptoamine ligand was exhaustively oxidized with either hot $HClO_4$ or hot HNO_3; neither $KClO_4$ nor $Cu(CH_3CN)_4ClO_4$ yielded a positive AgCl test under these conditions.

Attempts to solve the crystal structure of **3** have not been successful to date. Crystals of **3** exhibited apparent $6/mmm$ reciprocal lattice symmetry and extinctions consistent with the following space groups: $P6_3mc$ (No. 186), $P6_3/mmc$ (No. 194), and $P\bar{6}2c$ (No. 190). A data set was collected for a hexagonal unit cell of dimensions $a = b = 12.041$ (3) Å and $c = 22.42$ (1) Å. After extensive examination of the reciprocal lattice for evidence of twinning, a monoclinic cell of dimensions $a = 12.084$ (3) Å, $b = 20.912$ (8) Å, $c = 22.45$ (1) Å, and $\beta = 90.03$ (3)° was used to collect a second data set; however, solution in the monoclinic space group has also proven intractable thus far. All X-ray studies were performed by using a Syntex $P2_1$ automated diffractometer and graphite-monochromated Mo Kα radiation.

We have tentatively formulated **3** as $Cu_9[^-SC(CH_3)_2CH_2NH_3^+]_6\cdot6Cl\cdot3ClO_4$. This formulation is consistent with the presence of chloride and the elemental analyses below and, using the measured density, gives an integral number of formula units in both the hexagonal ($Z = 2$) and monoclinic ($Z = 4$) space groups.

Anal. Calcd for $Cu_9[^-SC(CH_3)_2CH_2NH_3^+]_6\cdot6Cl\cdot3ClO_4$ (**3**): Cu, 33.36; Cl, 18.62; S, 11.22; N, 4.90; C, 16.82; H, 3.88. Found: Cu, 33.64, Cl, 18.73; S, 10.97; N, 4.08; C, 16.40; H, 3.63.

4. Infrared Spectral Measurements. A Perkin-Elmer Model 225 spectrophotometer was used to obtain spectra of the complexes dispersed in KBr pellets. The absence of spectrally significant solute–matrix interactions was established by additional studies of the complexes dispersed as mineral oil and perfluorocarbon mulls.

5. Electronic Spectral Measurements. Electronic spectra were measured with Cary 14 and Cary 17 spectrophotometers equipped with quartz Dewars of standard design.

6. Magnetic Measurements. Variable-temperature (4.2–286 K) magnetic susceptibility data were collected with a Princeton Applied Research Model 150A vibrating-sample magnetometer operating at a field strength of 12.7–12.8 kG. Temperature control and measurement were accomplished with a calibrated GaAs diode. Susceptibilities were calibrated against a sample of $CuSO_4\cdot5H_2O$, which was run over the entire temperature range. The susceptibilities were corrected for diamagnetism.[10] EPR spectra of powdered samples were recorded on a Varian E-9 X-band spectrometer and a Varian E-15 Q-band spectrometer operating at ~9.1 and ~35 GHz, respectively. The X-band frequency was determined by using a Hewlett-Packard Model 5240A digital frequency meter. The Q-band frequency was obtained from the DPPH field position ($g = 2.0036$). X-Band spectra were recorded at ~300, ~80, and 9 K with the lowest temperature achieved with an Air Products Heli-tran liquid helium cooling system and measured with a calibrated carbon resistor. Q-Band spectra were taken at ~300 and ~110 K.

7. Collection of Diffraction Data for Complex 1. After observing a number of zero layer Weissenberg photographs (which revealed multiple diffraction spots) and noting difficulties in deducing a reasonably sized unit cell with autoindexing routines, it became obvious

(3) Thich, J. A.; Mastropaolo, D.; Potenza, J. A.; Schugar, H. J. *J. Am. Chem. Soc.* **1974**, *96*, 726–31 and references cited therein.
(4) Miyoshi, K.; Ishizu, K.; Sugiura, Y. *Chem. Lett.* **1976**, 669–72.
(5) Gergely, A.; Sovago, I. *Bioinorg. Chem.* **1978**, *9*, 47–60 and references cited therein.
(6) Schugar, H. J.; Ou, C. C.; Thich, J. A.; Potenza, J. A.; Lalancette, R. A.; Furey, W., Jr. *J. Am. Chem. Soc.* **1976**, *98*, 3047–8.
(7) Carroll, F. I.; White, J. D.; Wall, M. E. *J. Org. Chem.* **1963**, *28*, 1240–3.
(8) The purple cationic complex was bound to a cation-exchange resin. Sulfate was eluted and determined by titration.
(9) Hemmerich, P.; Sigwart, C. *Experientia* **1963**, *19*, 488–9.
(10) Mulay, L. N. In "Theory and Applications of Molecular Paramagnetism"; Boudreaux, E. A., Mulay, L. N., Eds.; Wiley: New York, 1976; pp 491–6.

Table I. Crystal Data for **1**

formula	$Cu_{14}[SC(CH_3)_2CH_2NH_2]_{12}Cl\cdot 3.5SO_4\cdot\sim 20H_2O$	d_{obsd}, g/cm^3	1.79 (1)
		d_{calcd}, g/cm^3	1.763
mol wt	2871.9	Z	4
a, Å	18.318 (3)	space group	$C2/c$
b, Å	21.826 (5)	μ, cm^{-1}	32.2
c, Å	28.829 (6)	λ, Å	0.710 69
β, deg	110.17 (1)	temp, °C	22 ± 1
V, Å^3	10819		

that crystals of complex **1** were aggregates. A large polycrystal was cleaved approximately in half along what appeared to be a possible twinning plane; the large crystal fragment obtained still exhibited the above difficulties. The smaller fragment, which showed no evidence of multiple spots, had dimensions of 0.50 × 0.40 × 0.40 mm and was mounted in a sealed capillary along with some DMF/H_2O mother liquor. The liquid was well removed from the crystal and completely eliminated the progressive decay in diffraction intensities observed for other crystals of **1** which were exposed to air. Unit cell constants (Table I) were determined at 22 ± 1 °C by a least-squares fit of 15 moderately intense high-angle reflections accurately centered on a Syntex $P2_1$ autodiffractometer using graphite-monochromated Mo Kα radiation (λ = 0.710 69 Å). A scan of the various classes of reflections revealed the following systematic absences: hkl, $h + k = 2n + 1$; $h0l$, $l = 2n + 1$. Two monoclinic space groups, $C2/c$ (C_{2h}^6, No. 15) and Cc (C_s^4, No. 9), are consistent with these extinctions. A crystal density of 1.79 (1) g/cm^3 was measured by using a gradient prepared from CCl_4 and $BrCH_2CH_2Br$ and calibrated[11] with Ni(acetate)$_2\cdot 4H_2O$ (d = 1.744 g/cm^3), $(NH_4)_2SO_4$ (d = 1.769 g/cm^3), $NH_4H_2PO_4$ (d = 1.803 g/cm^3), and $KCr(SO_4)_2\cdot 12H_2O$ (d = 1.826 g/cm^3). To minimize possible errors due to crystal dehydration, we made measurements on freshly prepared small crystals that were blotted dry of mother liquor and studied immediately. The crystals formed a well-defined layer whose position, relative to those of the standards, remained constant for at least 15 min.

Intensity data were collected at 22 ± 1 °C by using a θ–2θ scan to a maximum of 2θ = 70°. Each scan covered a range of 0.60° below the calculated Kα_1 position to 1.0° above the calculated Kα_2 position. An asymmetric scan range was chosen because diffraction peak profiles from this cleaved crystal showed some tailing at high angles. All data were collected by using a scan rate of 3.45° min^{-1}; stationary background counts were taken before and after each scan. The total time for background counting was equal to the scan time and was distributed equally before and after the peak. The intensities of three standard reflections were recorded after every 47 reflections and showed random variations of ±2%. A total of 4790 unique reflections out of a possible 18887 had $I > 3\sigma(I)$ and were considered observed. Intensities (I) and their standard deviation ($\sigma(I)$) were calculated from the relationships $I = (P - LB - HB)SR$ and $\sigma(I) = (P + LB + HB)^{1/2}SR$, where P is the peak count, LB and HB are the low and high angle backgrounds, respectively, and SR is the scan rate. All intensities were corrected for decay and for Lorentz and polarization effects; the polarization correction for the parallel–parallel mode of the $P2_1$ diffractometer was used by assuming the monochromator crystal to be 50% perfect and 50% mosaic. Absorption corrections were applied; transmission factors ranged from 0.317 to 0.504 with a linear absorption coefficient of 32.2 cm^{-1} for Mo Kα radiation.

8. Solution and Refinement of the Structure.[12] The structure was solved by direct methods. The initial assumption of space group $C2/c$ resulted in a satisfactory solution and refinement of the structure. The alternate choice of space group (Cc) was not explored because the additional computing costs would have been prohibitive. Approximate coordinates for the central atom in the cluster (later assigned as Cl), the seven unique copper atoms, and the six mercaptide sulfur atoms were revealed by an E map calculated by using phases from the solution having the highest figure of merit obtained from the program MULTAN.[13] A series of structure factor and difference Fourier calculations revealed the remaining nonhydrogen atoms of the cluster as well as one lattice SO_4 group. At this stage, further progress with the solution of the structure depended upon locating and assigning the missing lattice species, as well as assigning the central ion of the cluster.

For help in locating the missing ions, isotropic full-matrix least-squares refinement was initiated by using neutral atom scattering factors from Cromer and Waber.[14] Both real and imaginary parts of the anomalous dispersion correction were applied to Cu, S, and Cl atoms.[15] Refinement was based on F and unit weights were used initially. Several cycles of isotropic refinement reduced $R_F = \sum||F_o| - |F_c||/\sum|F_o|$ to 0.19. A difference Fourier map prepared at this point revealed numerous possible positions for the missing lattice species.

To assign these species, we utilized analytical, infrared, and chemical data obtained for **1** and the closely related copper–penicillamine cluster. The chemistry of the penicillamine cluster strongly indicated that its formation was dependent upon the presence of chloride ion.[5] We obtained a positive AgCl test for **1** after the complex was oxidized in either hot $HClO_4$ or HNO_3. This procedure serves to destroy the mercaptide ligand which otherwise would strongly bind Ag^+. The amount of Cl observed (1.26%) corresponded to one Cl per cluster. The special role of Cl in the formation of the copper–penicillamine cluster combined with the analytical data for **1** suggested that Cl was the central ion. The choice between Cl^- or S^{2-} as the central ion could not be resolved by purely crystallographic methods.

The presence of SO_4 in **1** was revealed clearly by intense infrared absorptions at ~1120 and 616 cm^{-1}. In addition to the total sulfur in **1**, the amount of sulfur present as sulfate was required to determine the number of lattice sulfate groups. This information was obtained by using an analytical technique which combined ion-exchange and titration procedures.[8] Finally, the observed copper coordination geometries suggested the presence of eight cuprous and six cupric species per cluster. A stoichiometry for **1** (two asymmetric units) which satisfies the analytical and spectroscopic data, maintains charge balance, and gives an integral number of formula units per unit cell is $[Cu^I_8Cu^{II}_6(SC(CH_3)_2CH_2NH_2)_{12}Cl]^{7+}\cdot 3.5SO_4\cdot 20H_2O$. Thus, 10 lattice H_2O molecules and 0.75 SO_4^{2-} groups per asymmetric unit were missing. Examination of the difference Fourier map revealed ten peaks, assigned as oxygen, whose refined isotropic temperature factors ranged from 13 to 26 Å^2. We were unable to locate the remaining fractional sulfate ion. The sulfate group which was located is involved in a tight and extensive hydrogen bonding network with surrounding lattice H_2O molecules (Table IV). Presumably, a disorder exists between the missing SO_4 group and the lattice H_2O molecules. We note that comparable disorders were encountered in the solution of an anionic copper–penicillamine cluster.[2] In that structure, disorder involving the lattice H_2O molecules and the Tl^+ gegenions could not be removed by remeasuring the diffraction data at 105 K and did not allow the ultimate R_F to drop below 0.17.

Anisotropic thermal parameters for the Cu, S, and Cl atoms were used in further refinements. A weighting scheme, chosen by an analysis of variance, led to the following choices for $\sigma(F_o)$:

$$\sigma(F_o) = 9.47 - 0.202|F_o|; \quad |F_o| \le 26.2$$

$$\sigma(F_o) = 3.00 + 0.045|F_o|; \quad 26.2 \le |F_o| \le 43.5$$

$$\sigma(F_o) = 1.96 + 0.069|F_o|; \quad |F_o| > 43.5$$

Because of the disorder problem, the large amount of data, and the large number of parameters involved, only isotropic thermal parameters were used and refined for the mercaptoamine ligands and oxygen atoms. Full-matrix refinement of 174 positional parameters and 134 temperature factors led to convergence with R_F = 0.10 and $R_{wF} = [\sum w(F_o - F_c)^2/\sum wF_o^2]^{1/2}$ = 0.14. For the last cycle, all parameter changes were within their estimated standard deviation. A final difference map showed a general background of approximately 1 e/Å^3. Final atomic positional and thermal parameters are given in Table II. Views of the structure showing the atom numbering scheme are given in Figures 1 and 2; the packing of the structure is shown in Figure

(11) Weast, R. C., Ed., "Handbook of Chemistry and Physics", 53rd ed; Chemical Rubber Publishing Co.: Cleveland, OH, 1972.
(12) In addition to local programs for the IBM 360/67 computer, local modifications of the following programs were employed: Coppen's ABSORB program; Zalkin's FORDAP Fourier program; Johnson's ORTEP II thermal ellipsoid plotting program; Busing, Martin, and Levy's ORFEE error function and ORFLS least-squares programs. The analysis of variance was carried out by using program NANOVA obtained from Professor I. Bernal: see Ricci, J. S.; Eggers, C. A.; Bernal, I. *Inorg. Chim. Acta* **1972**, *6*, 97–105.
(13) Program MULTAN: Main, P.; Woolfson, M. M.; Germain, G., Department of Physics, University of York, England.
(14) Cromer, D. T.; Waber, J. T. *Acta Crystallogr.* **1965**, *18*, 104–9.
(15) "International Tables for X-Ray Crystallography;" Kynoch Press: Birmingham, England, 1962; Vol. III, pp 201–13.

Table II. Fractional Atomic Coordinates and Thermal Parameters[a] for **1**

atom	*x*	*y*	*z*	β_{11}	β_{22}	β_{33}	β_{12}	β_{13}	β_{23}
Cu(1)	0.3527 (1)	0.3508 (1)	0.50239 (9)	26.1 (7)	18.0 (6)	12.0 (4)	2.4 (5)	5.3 (5)	−0.6 (4)
Cu(2)	0.1633 (1)	0.3622 (1)	0.48524 (9)	27.4 (7)	19.5 (6)	11.2 (4)	−1.3 (6)	6.3 (4)	−0.6 (4)
Cu(3)	0.3138 (1)	0.2353 (1)	0.42333 (9)	26.0 (7)	18.0 (6)	12.7 (4)	1.2 (6)	4.6 (5)	−0.1 (4)
Cu(4)	0.1251 (1)	0.2456 (1)	0.40717 (9)	27.2 (7)	17.5 (5)	12.1 (4)	0.9 (6)	6.7 (4)	−0.6 (4)
Cu(5)	−0.0220 (1)	0.2679 (1)	0.4746 (1)	18.4 (6)	18.9 (6)	18.3 (5)	−1.0 (5)	7.0 (5)	−4.4 (4)
Cu(6)	0.1992 (1)	0.0831 (1)	0.38702 (9)	28.8 (8)	17.2 (5)	12.1 (4)	1.2 (6)	4.8 (4)	−4.5 (4)
Cu(7)	0.2186 (1)	0.3942 (1)	0.37040 (8)	27.1 (7)	20.5 (6)	9.8 (3)	1.5 (6)	4.7 (4)	4.4 (3)
S(1)	0.3224 (3)	0.3394 (2)	0.41935 (17)	19.8 (13)	17.7 (11)	11.9 (8)	0 (1)	6.9 (8)	2.5 (7)
S(2)	0.1331 (3)	0.3502 (2)	0.40178 (17)	21.7 (13)	16.3 (10)	9.6 (7)	4 (1)	4.6 (8)	2.9 (6)
S(3)	0.2018 (3)	0.1871 (2)	0.37691 (16)	26.6 (15)	16.7 (11)	7.9 (7)	3 (1)	3.8 (8)	−1.8 (6)
S(4)	0.0461 (3)	0.2013 (2)	0.44398 (17)	16.5 (12)	17.2 (11)	10.1 (7)	−1 (1)	2.9 (8)	−1.7 (7)
S(5)	0.0856 (3)	0.3194 (2)	0.52346 (16)	18.3 (13)	16.2 (10)	10.7 (7)	3 (1)	5.7 (8)	−1.6 (7)
S(6)	0.2243 (3)	0.0888 (2)	0.46967 (18)	24.7 (14)	13.9 (10)	11.7 (7)	0 (1)	5.0 (9)	−1.7 (7)
Cl	1/4	1/4	1/2	20.8 (17)	12.7 (13)	8.1 (9)	0 (1)	5.4 (10)	0.2 (8)
S(8)	0.2031 (5)	0.4656 (4)	0.2135 (3)	60 (3)	39 (2)	18.2 (12)	−22 (2)	7.8 (16)	0.9 (12)

atom	*x*	*y*	*z*	*B*, Å^2	atom	*x*	*y*	*z*	*B*, Å^2
N(1)	0.297 (2)	0.4384 (19)	0.3452 (14)	12.1 (8)	C(52)	0.0382 (11)	0.3725 (10)	0.5534 (7)	3.6 (4)
C(11)	0.383 (2)	0.4372 (16)	0.3851 (12)	7.2 (7)	C(53)	0.010 (3)	0.328 (3)	0.587 (2)	13 (1)
C(12)	0.3962 (11)	0.3668 (10)	0.3946 (7)	3.6 (4)	C(54)	0.086 (3)	0.422 (2)	0.5732 (16)	11 (1)
C(13)	0.476 (2)	0.3499 (16)	0.4261 (12)	7.7 (8)	N(6)	0.2167 (12)	−0.0071 (10)	0.3962 (8)	5.2 (4)
C(14)	0.385 (2)	0.3379 (16)	0.3453 (12)	7.7 (7)	C(61)	0.2558 (14)	−0.0283 (12)	0.4499 (9)	5.3 (5)
N(2)	0.1273 (11)	0.4413 (9)	0.3235 (7)	4.4 (4)	C(62)	0.2195 (12)	0.0040 (10)	0.4825 (8)	3.9 (4)
C(21)	0.0532 (13)	0.4070 (11)	0.3140 (8)	4.3 (4)	C(63)	0.1338 (12)	−0.0145 (11)	0.4698 (8)	4.2 (4)
C(22)	0.0423 (11)	0.3881 (10)	0.3635 (7)	3.7 (4)	C(64)	0.2679 (16)	−0.0089 (14)	0.5348 (10)	6.3 (6)
C(23)	0.0233 (14)	0.4434 (12)	0.3895 (9)	5.0 (5)	O(1)	0.1878 (12)	0.4564 (10)	0.1624 (8)	7.7 (5)
C(24)	−0.0263 (15)	0.3414 (13)	0.3514 (10)	5.9 (6)	O(2)	0.245 (2)	0.5194 (17)	0.2325 (12)	13.1 (9)
N(3)	0.1557 (12)	0.0772 (11)	0.3126 (8)	5.6 (5)	O(3)	0.138 (2)	0.4631 (15)	0.2285 (11)	12.4 (8)
C(31)	0.1220 (16)	0.1347 (13)	0.2881 (10)	6.0 (6)	O(4)	0.238 (2)	0.414 (2)	0.2426 (15)	17 (1)
C(32)	0.1789 (12)	0.1871 (10)	0.3092 (8)	4.0 (4)	O(5)	0.237 (2)	0.0708 (16)	0.1795 (12)	12.6 (9)
C(33)	0.142 (2)	0.2463 (16)	0.2870 (12)	7.8 (8)	O(6)	0.405 (3)	0.072 (2)	0.1533 (16)	18 (1)
C(34)	0.250 (2)	0.176 (2)	0.2971 (13)	8.7 (9)	O(7)	0.449 (2)	0.081 (2)	0.2835 (14)	15 (1)
N(4)	−0.1198 (16)	0.2262 (13)	0.4303 (10)	7.7 (6)	O(8)	0.186 (2)	0.3559 (15)	0.1068 (12)	12.7 (9)
C(41)	−0.099 (2)	0.196 (2)	0.3821 (13)	8.5 (8)	O(9)	0.334 (4)	0.307 (3)	0.072 (2)	26 (2)
C(42)	−0.0360 (11)	0.1555 (9)	0.4040 (7)	3.4 (4)	O(10)	0.305 (4)	0.176 (3)	0.121 (2)	26 (2)
C(43)	−0.060 (2)	0.107 (2)	0.4361 (15)	10 (1)	O(11)	0.424 (3)	0.209 (3)	0.272 (2)	24 (2)
C(44)	−0.013 (3)	0.119 (2)	0.3698 (16)	11 (1)	O(12)	0.085 (4)	−0.017 (3)	0.230 (2)	25 (2)
N(5)	−0.0861 (16)	0.3285 (14)	0.4954 (10)	7.8 (6)	O(13)	0.452 (3)	0.463 (2)	0.167 (2)	17 (1)
C(51)	−0.038 (2)	0.396 (2)	0.5156 (15)	10 (1)	O(14)	0.419 (4)	0.261 (3)	0.165 (2)	25 (2)

[a] Anisotropic temperature factors are $\times 10^4$ and are of the form $\exp[-(\beta_{11}h^2 + \beta_{22}k^2 + \beta_{33}l^2 + 2\beta_{12}hk + 2\beta_{13}hl + 2\beta_{23}kl)]$.

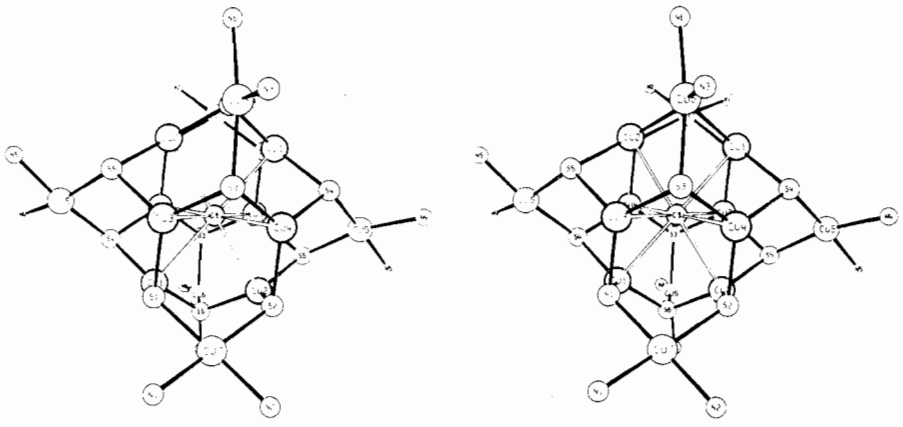

Figure 1. Stereoscopic view of the $Cu^I_8Cu^{II}_6S_{12}N_{12}Cl$ cluster framework. For clarity the ligand carbon atoms and lattice H_2O and SO_4^{2-} species have been omitted.

3. A list of observed and calculated structure factors is available.[16]

Description of the Structure

The structure consists of discrete, centrosymmetric $Cu^I_8Cu^{II}_6[SC(CH_3)_2CH_2NH_2]_{12}Cl^{7+}$ clusters in which 14 copper ions are linked by 12 three-coordinate mercaptide ions and an eight-coordinate chloride ion. Structural features of this complex correspond closely to those reported for the higher symmetry, anionic $Cu_{14}[SC(CH_3)_2CH(CO_2)NH_2]_{12}Cl^{5-}$ cluster complex which is derived from the parent D-penicillamine^{2-} ligand and which crystallized in the cubic space group $F432$.[2] Both structures have a common $Cu_{14}S_{12}Cl$ core.

The core consists of a distorted icosahedral arrangement of 12 sulfur atoms [S(1)–S(6) and S(1′)–S(6′)] with 8 of the 20 triangular icosahedral faces occupied by copper ions [Cu(1)–Cu(4) and Cu(1′)–Cu(4′)] which form an approximate cube. The single chloride ion lies at the common center of the icosahedron and of the cube and is bound to the 8 copper ions in the antifluorite manner. The close approximation of these 8 copper ions to a cubic arrangement is indicated by the

(16) Supplementary material.

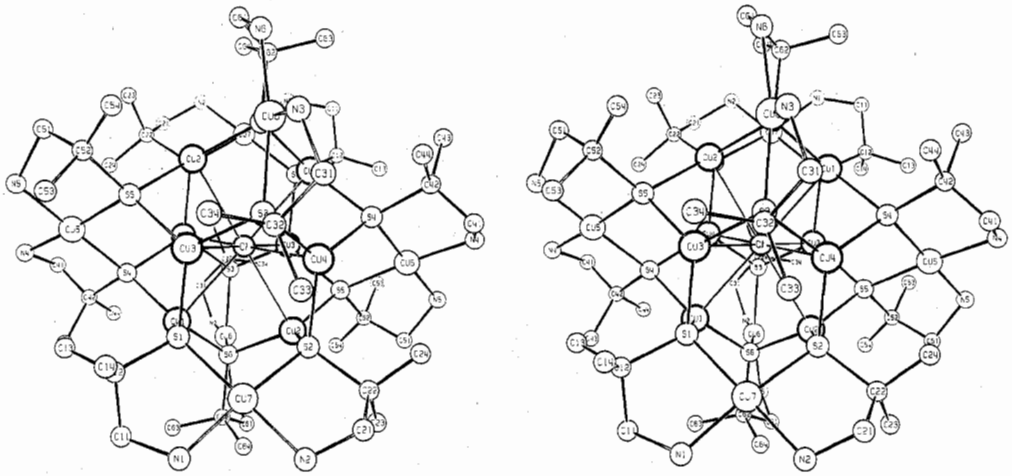

Figure 2. Stereoscopic view of the cluster showing the carbon atoms and the atom numbering scheme. For clarity the H_2O and SO_4^{2-} species have been omitted.

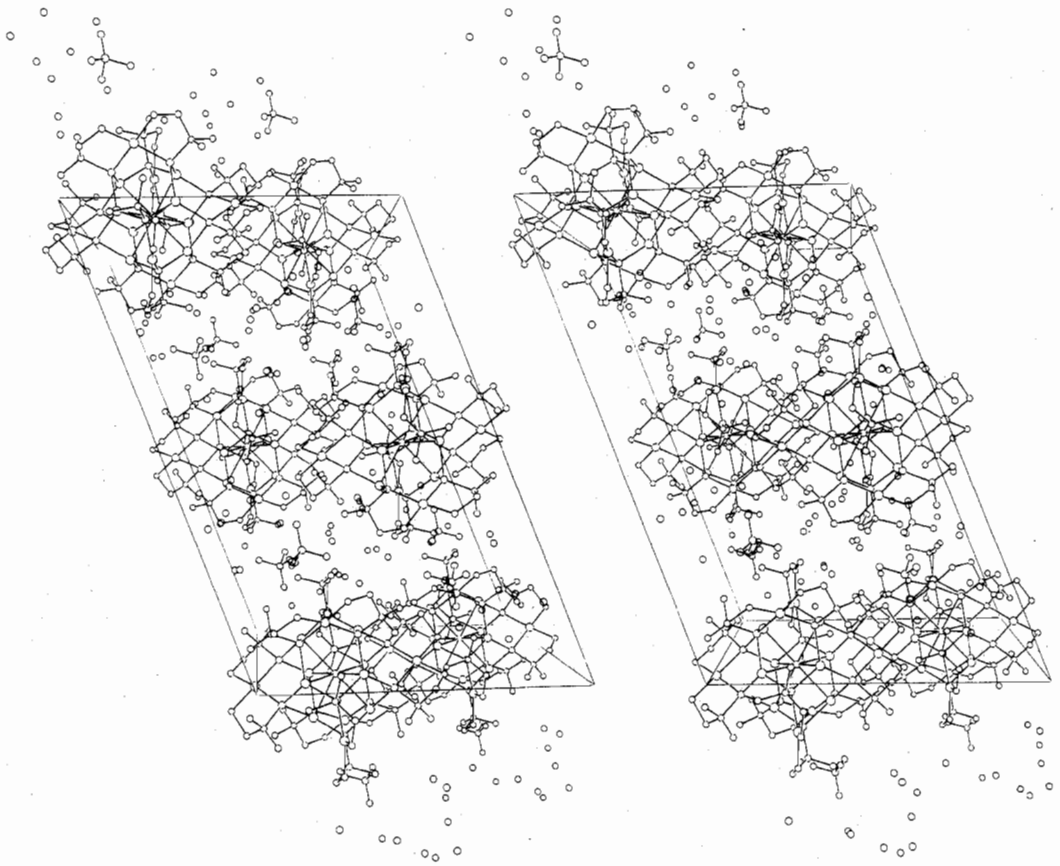

Figure 3. Stereoscopic packing diagram of **1** viewed along *b*; the *a* axis is horizontal. The box delineates one unit cell.

Cu···Cu distances which vary from 3.264 (4) to 3.341 (3) Å and by the Cl–Cu–Cl angles which vary from 69.31 (7) to 71.34 (7)° (the ideal value is 70.53°). The remaining 6 core copper ions [Cu(5)–Cu(7) and Cu(5′)–Cu(7′)] are located approximately along 6 of the 30 icosahedron edges and form a distorted octahedral array with Cu···Cu distances ranging from 6.645 (4) to 6.825 (4) Å.

Each of the two structurally distinct types of copper atoms within the core is four-coordinate. Those comprising the inner cubic arrangement have an S_3Cl donor set. The chloride ion is rather weakly bound and is oriented approximately normal to each triangular planar CuS_3 unit; S–Cu–S bond angles within these triangular units span the range 117.9 (2)–121.1 (2)° while the Cl–Cu–S angles vary from 88.3 (1) to 90.6 (1)°. Observed Cu–Cl distances (2.852 (3)–2.880 (3) Å) exceed significantly the sum of the single bond covalent radii (2.41 Å). To help assign the oxidation state of these ions, we have drawn comparisons with structural features reported for a monomeric cuprous complex with a triangular ClS_2 donor set. The observed Cu–Cl and Cu–S(thiouracil) distances were 2.260 (1) Å, and 2.228 (1) and 2.225 (1) Å, respectively.[17] In comparison, Cu–S distances within the CuS_3Cl units of **1** range from 2.268 (5) to 2.297 (5) Å; thus, the copper ions comprising the inner cubic arrangement in **1** may be viewed as having a tightly bound triangular S_3 donor set along with a weakly bound, apical chloride ion. Dominant triangular planar coordination geometry is characteristic both of cuprous

(17) Hunt, G. W.; Griffith, E. A. H.; Amma, E. L. *Inorg. Chem.* **1976**, *15*, 2993–7.

Table III. Bond Distances (Å) and Angles (Deg)[a] in **1**

Cu(1)–S(1)	2.277 (6)	Cu(5)–S(5)	2.285 (5)	Cu(1)···Cu(2)	3.341 (3)	Cu(2)···Cu(3′)	3.301 (4)
Cu(1)–S(4′)	2.268 (5)	Cu(5)–S(4)	2.283 (6)	Cu(1)···Cu(3)	3.306 (4)	Cu(2)···Cu(4)	3.309 (4)
Cu(1)–S(6′)	2.272 (6)	Cu(5)–N(4)	2.02 (3)	Cu(1)···Cu(4′)	3.264 (4)	Cu(3)···Cu(4)	3.331 (3)
Cu(1)–Cl	2.880 (3)	Cu(5)–N(5)	1.99 (3)	N(1)–C(11)	1.60 (4)	N(4)–C(41)	1.69 (5)
Cu(2)–S(2)	2.290 (5)	Cu(6)–S(3)	2.292 (6)	C(11)–C(12)	1.58 (4)	C(41)–C(42)	1.42 (4)
Cu(2)–S(5)	2.279 (6)	Cu(6)–S(6)	2.269 (6)	C(12)–C(13)	1.48 (3)	C(42)–C(43)	1.57 (5)
Cu(2)–S(6′)	2.287 (5)	Cu(6)–N(3)	2.02 (2)	C(12)–C(14)	1.50 (4)	C(42)–C(44)	1.44 (5)
Cu(2)–Cl	2.870 (3)	Cu(6)–N(6)	2.00 (2)	C(12)–S(1)	1.83 (2)	C(42)–S(4)	1.84 (2)
Cu(3)–S(1)	2.281 (6)	Cu(7)–S(1)	2.277 (5)	N(2)–C(21)	1.49 (3)	N(5)–C(51)	1.71 (5)
Cu(3)–S(3)	2.283 (5)	Cu(7)–S(2)	2.275 (6)	C(21)–C(22)	1.56 (3)	C(51)–C(52)	1.53 (4)
Cu(3)–S(5′)	2.286 (5)	Cu(7)–N(2)	2.03 (2)	C(22)–C(23)	1.52 (4)	C(52)–C(53)	1.60 (6)
Cu(3)–Cl	2.852 (3)	Cu(7)–N(1)	2.05 (4)	C(22)–C(24)	1.56 (3)	C(52)–C(54)	1.39 (5)
Cu(4)–S(2)	2.297 (5)	S(8)–O(1)	1.42 (2)	C(22)–S(2)	1.84 (2)	C(52)–S(5)	1.83 (2)
Cu(4)–S(3)	2.282 (6)	S(8)–O(2)	1.40 (3)	N(3)–C(31)	1.47 (3)	N(1)–C(61)	1.54 (3)
Cu(4)–S(4)	2.284 (6)	S(8)–O(3)	1.40 (4)	C(31)–C(32)	1.53 (3)	C(61)–C(62)	1.50 (4)
Cu(4)–Cl	2.861 (2)	S(8)–O(4)	1.43 (4)	C(32)–C(33)	1.50 (4)	C(62)–C(63)	1.54 (3)
				C(32)–C(34)	1.48 (5)	C(62)–C(64)	1.49 (3)
				C(32)–S(3)	1.85 (2)	C(62)–S(6)	1.89 (2)
S(1)–Cu(1)–S(4′)	120.5 (2)	S(4)–Cu(5)–S(5)	94.6 (2)	Cu(3)–S(3)–Cu(4)	93.7 (2)	Cu(1′)–S(6)–Cu(2′)	94.3 (2)
S(1)–Cu(1)–S(6′)	118.7 (2)	N(4)–Cu(5)–N(5)	90.2 (12)	Cu(3)–S(3)–Cu(6)	115.9 (2)	Cu(1′)–S(6)–Cu(6)	118.6 (2)
S(4′)–Cu(1)–S(6′)	120.7 (2)	S(4)–Cu(5)–N(4)	87.2 (9)	Cu(4)–S(3)–Cu(6)	117.6 (3)	Cu(2′)–S(6)–Cu(6)	116.0 (3)
S(1)–Cu(1)–Cl	88.3 (1)	S(4)–Cu(5)–N(5)	175.0 (8)	Cu(3)–S(3)–C(32)	116.7 (8)	Cu(1′)–S(6)–C(62)	115.0 (8)
S(4′)–Cu(1)–Cl	90.4 (2)	S(5)–Cu(5)–N(4)	177.3 (8)	Cu(4)–S(3)–C(32)	117.2 (7)	Cu(2′)–S(6)–C(62)	116.1 (1)
S(6′)–Cu(1)–Cl	88.4 (2)	S(5)–Cu(5)–N(5)	87.8 (8)	Cu(6)–S(3)–C(32)	97.3 (7)	Cu(6)–S(6)–C(62)	98.4 (7)
S(2)–Cu(2)–S(5)	119.7 (2)	S(3)–Cu(6)–S(6)	94.2 (2)	Cu(2)–Cu(1)–Cu(3)	89.35 (8)	Cu(1)–Cu(3)–Cu(2′)	90.19 (9)
S(2)–Cu(2)–S(6′)	119.7 (2)	N(3)–Cu(6)–N(6)	93.7 (9)	Cu(2)–Cu(1)–Cu(4′)	90.19 (8)	Cu(1)–Cu(3)–Cu(4)	90.71 (9)
S(5)–Cu(2)–S(6)	120.5 (2)	S(3)–Cu(6)–N(3)	86.9 (7)	Cu(3)–Cu(1)–Cu(4′)	89.87 (9)	Cu(2′)–Cu(3)–Cu(4)	89.72 (9)
S(2)–Cu(2)–Cl	88.8 (1)	S(3)–Cu(6)–N(6)	169.7 (7)	Cu(1)–Cu(2)–Cu(3′)	89.65 (8)	Cu(1′)–Cu(4)–Cu(2)	90.77 (9)
S(5)–Cu(2)–Cl	89.1 (1)	S(6)–Cu(6)–N(3)	169.2 (7)	Cu(1)–Cu(2)–Cu(4)	90.47 (9)	Cu(1′)–Cu(4)–Cu(3)	90.45 (8)
S(6′)–Cu(2)–Cl	88.4 (1)	S(6)–Cu(6)–N(6)	87.1 (6)	Cu(3)–Cu(2)–Cu(4)	89.18 (9)	Cu(2)–Cu(4)–Cu(3)	89.47 (8)
S(1)–Cu(3)–S(3)	119.5 (2)	S(1)–Cu(7)–S(2)	94.3 (2)	Cu(7)–N(1)–C(11)	112 (3)	Cu(5)–N(4)–C(41)	107 (2)
S(1)–Cu(3)–S(5′)	120.0 (2)	N(1)–Cu(7)–N(2)	92.3 (12)	N(1)–C(11)–C(12)	102 (2)	N(4)–C(41)–C(42)	105 (2)
S(3)–Cu(3)–S(5′)	120.4 (2)	S(1)–Cu(7)–N(1)	86.2 (10)	C(11)–C(12)–C(13)	115 (2)	C(41)–C(42)–C(43)	110 (3)
S(1)–Cu(3)–Cl	88.9 (2)	S(1)–Cu(7)–N(2)	176.9 (7)	C(11)–C(12)–C(14)	107 (2)	C(41)–C(42)–C(44)	115 (3)
S(3)–Cu(3)–Cl	88.9 (2)	S(2)–Cu(7)–N(1)	176.3 (12)	C(11)–C(12)–S(1)	107 (2)	C(41)–C(42)–S(4)	107 (2)
S(5′)–Cu(3)–Cl	89.4 (2)	S(2)–Cu(7)–N(2)	87.5 (6)	C(13)–C(12)–C(14)	105 (2)	C(43)–C(42)–C(44)	104 (3)
S(2)–Cu(4)–S(3)	117.9 (2)	Cu(1)–Cl–Cu(2)	71.05 (7)	C(13)–C(12)–S(1)	113 (2)	C(43)–C(42)–S(4)	109 (2)
S(2)–Cu(4)–S(4)	121.1 (2)	Cu(1)–Cl–Cu(3)	70.45 (7)	C(14)–C(12)–S(1)	110 (2)	C(44)–C(42)–S(4)	111 (2)
S(3)–Cu(4)–S(4)	120.9 (2)	Cu(1′)–Cl–Cu(4)	69.31 (7)	Cu(7)–N(2)–C(21)	111 (1)	Cu(5)–N(5)–C(51)	113 (2)
S(2)–Cu(4)–Cl	88.9 (1)	Cu(2)–Cl–Cu(3′)	70.46 (7)	N(2)–C(21)–C(22)	111 (2)	N(5)–C(51)–C(52)	101 (3)
S(3)–Cu(4)–Cl	88.7 (1)	Cu(2′)–Cl–Cu(4′)	70.55 (7)	C(21)–C(22)–C(23)	111 (2)	C(51)–C(52)–C(53)	103 (3)
S(4)–Cu(4)–Cl	90.6 (1)	Cu(3)–Cl–Cu(4)	71.34 (7)	C(21)–C(22)–C(24)	108 (2)	C(51)–C(52)–C(54)	109 (3)
Cu(1)–S(1)–Cu(3)	93.0 (2)	Cu(1′)–S(4)–Cu(4)	91.6 (2)	C(21)–C(22)–S(2)	107 (2)	C(51)–C(52)–S(5)	110 (2)
Cu(1)–S(1)–Cu(7)	116.3 (2)	Cu(1′)–S(4)–Cu(5)	118.9 (2)	C(23)–C(22)–C(24)	109 (2)	C(53)–C(52)–C(54)	121 (3)
Cu(3)–S(1)–Cu(7)	119.8 (2)	Cu(4)–S(4)–Cu(5)	115.4 (2)	C(23)–C(22)–S(2)	112 (1)	C(53)–C(52)–S(5)	102 (2)
Cu(1)–S(1)–C(12)	115.3 (6)	Cu(1′)–S(4)–C(42)	117.0 (7)	C(24)–C(22)–S(2)	109 (2)	C(54)–C(52)–S(5)	111 (3)
Cu(3)–S(1)–C(12)	114.7 (7)	Cu(4)–S(4)–C(42)	116.7 (7)	Cu(6)–N(3)–C(31)	114 (2)	Cu(6)–N(6)–C(61)	115 (2)
Cu(7)–S(1)–C(12)	99.1 (6)	Cu(5)–S(4)–C(42)	98.7 (7)	N(3)–C(31)–C(32)	110 (2)	N(6)–C(61)–C(62)	110 (2)
Cu(2)–S(2)–Cu(4)	92.3 (2)	Cu(2)–S(5)–Cu(3′)	92.6 (2)	C(31)–C(32)–C(33)	109 (2)	C(61)–C(62)–C(63)	111 (2)
Cu(2)–S(2)–Cu(7)	114.8 (2)	Cu(2)–S(5)–Cu(5)	117.0 (2)	C(31)–C(32)–C(34)	108 (2)	C(61)–C(62)–C(64)	108 (2)
Cu(4)–S(2)–Cu(7)	120.9 (2)	Cu(3′)–S(5)–Cu(5)	118.8 (2)	C(31)–C(32)–S(3)	107 (2)	C(61)–C(62)–S(6)	106 (2)
Cu(2)–S(2)–C(22)	114.8 (8)	Cu(2)–S(5)–C(52)	116.4 (7)	C(33)–C(32)–C(34)	111 (3)	C(63)–C(62)–C(64)	113 (2)
Cu(4)–S(2)–C(22)	114.9 (7)	Cu(3′)–S(5)–C(52)	114.7 (6)	C(33)–C(32)–S(3)	111 (2)	C(63)–C(62)–S(6)	109 (1)
Cu(7)–S(2)–C(22)	100.2 (8)	Cu(5)–S(5)–C(52)	98.7 (6)	C(34)–C(32)–S(3)	111 (2)	C(64)–C(62)–S(6)	109 (2)
				O(1)–S(8)–O(2)	114 (2)		
				O(1)–S(8)–O(3)	116 (2)		
				O(1)–S(8)–O(4)	113 (2)		
				O(2)–S(8)–O(3)	109 (2)		
				O(2)–S(8)–O(4)	111 (2)		
				O(3)–S(8)–O(4)	92 (2)		

[a] Primed atoms are related to unprimed atoms by the symmetry operation $^1/_2 - x$, $^1/_2 - y$, $1 - z$.

ion sites in sulfide mineral structures[18] and of cuprous complexes and indicates that Cu(1)–Cu(4) are cuprous species.

The remaining six core copper ions [Cu(5)–Cu(7)] have an approximately planar cis S_2N_2 ligand set which suggests that they are cupric species. Observed Cu–N and Cu–S distances span the ranges 1.99 (3)–2.05 (5) and 2.269 (6)–2.292 (6) Å, respectively. The Cu–N values lie within the range commonly observed for Cu^{II}–N bond lengths.[19] Comparisons with copper(II) mercaptides are restricted by the well-known redox instability of nearly all such complexes. A Cu^{II}–S(mercaptide) distance of 2.359 (4) Å has been reported for an approximately trigonal-bipyramidal CuN_4S(mercaptide) chromophore.[20] Although a copper protein which exhibits Cu^{II}–S(mercaptide) bonding has been characterized crystallographically,[21] Cu–

(18) Nickless, G., Ed., "Inorganic Sulfur Chemistry"; Elsevier: New York, 1968; pp 724–6.

(19) Ou, C. C.; Miskowski, V. M.; Lalancette, R. A.; Potenza, J. A.; Schugar, H. J. *Inorg. Chem.* **1976**, *15*, 3157–61.

(20) Hughey, J. L., IV; Fawcett, T. G.; Rudich, S. M.; Lalancette, R. A.; Potenza, J. A.; Schugar, H. J. *J. Am. Chem. Soc.* **1979**, *101*, 2617–23.

Table IV. Possible Hydrogen Bonding Contacts[a] in **1**

atoms[b]	distance, Å	atoms[b]	distance, Å
O(5)···O(2) i	2.69	O(9)···O(14)	2.77
O(5)···N(1) i	2.99	O(10)···O(14)	2.75
O(6)···O(7) ii	2.68	O(11)···O(14) ii	3.04
O(6)···O(10)	2.86	O(12)···O(13) iv	2.52
O(6)···N(2) i	3.04	O(12)···O(2) i	3.04
O(7)···O(11)	2.84	O(12)···N(3)	3.07
O(7)···O(3) i	2.98	O(13)···N(6) v	3.07
O(7)···O(7) ii	3.12	O(1)···N(6) v	2.93
O(8)···O(1)	2.71	O(2)···N(3) v	2.87
O(8)···O(5) iii	2.94	O(3)···N(2)	2.85
O(8)···N(4) iii	3.12	O(4)···N(1)	2.83

[a] Only distances less than 3.2 Å are listed. [b] i = $^1/_2 - x, -^1/_2 + y, ^1/_2 - z$; ii = $1 - x, y, ^1/_2 - z$; iii = $\bar{x}, y, ^1/_2 - z$; iv = $-^1/_2 + x, -^1/_2 + y, z$; v = $^1/_2 - x, ^1/_2 + y, ^1/_2 - z$.

ligand distances have not been reported. Equatorial bonding of thioether ligands in various tetragonal and square-pyramidal Cu(II) complexes has yielded Cu(II)–S distances in the range 2.30–2.45 Å.[19]

Structural parameters of the six crystallographically unique $SC(CH_3)_2CH_2NH_2$ ligands are uneventful. Within the observed limits of error, they correspond reasonably well to those reported for a $Co[SC(CH_3)_2CH_2NH_2]_2$ complex.[22] The lattice water molecules, the sulfate oxygen atoms [O(1)–O(4)], and the amino nitrogen atoms are involved in an extensive hydrogen bonding network (Table IV) which serves to stabilize the structure.

Distances between the cuprous ions in **1** (3.264 (4)–3.341 (3) Å) are substantially longer than those (2.76–2.91 Å) reported for three copper(I)–thiolate complexes which form chloride-free $Cu_8S_{12}^{4-}$ substructures.[23,24] A recent molecular orbital study of the $Cu_8S_{12}^{4-}$ cluster indicated that direct Cu···Cu bonding does not play an important structural role.[25] However, other workers have argued on crystallographic grounds that the stability of the $Cu_8S_{12}^{4-}$ cluster results in part from Cu···Cu bonding.[24] In any event, direct Cu···Cu bonding must be attenuated strongly in the $[Cu_8S_{12}Cl]^{5-}$ substructure of **1**.

Results and Discussion

Magnetic Susceptibility Theory. Magnetic exchange interactions within the cluster can be described by the isotropic spin Hamiltonian

$$\hat{H} = -2J\sum_{i<j}\hat{S}_i\cdot\hat{S}_j \qquad (1)$$

where the exchange parameter is assumed to be equal for any nearest-neighbor Cu(II)–Cu(II) pair in the complex. If the six Cu(II) ions are assumed to occupy the vertices of a regular octahedron, the magnetic susceptibility can be derived by following a generalized procedure.[26]

The spin Hamiltonian operator representing the isotropic magnetic exchange interaction between nearest-neighbor Cu(II) ion is written as

$$\hat{H} = -2J[\hat{S}_1\cdot\hat{S}_2 + \hat{S}_1\cdot\hat{S}_3 + \hat{S}_1\cdot\hat{S}_4 + \hat{S}_1\cdot\hat{S}_5 + \hat{S}_2\cdot\hat{S}_3 + \hat{S}_2\cdot\hat{S}_5 + \hat{S}_2\cdot\hat{S}_6 + \hat{S}_3\cdot\hat{S}_4 + \hat{S}_3\cdot\hat{S}_6 + \hat{S}_4\cdot\hat{S}_5 + \hat{S}_4\cdot\hat{S}_6 + \hat{S}_5\cdot\hat{S}_6] \qquad (2)$$

It is convenient to define the total spin (S) for any state of the cluster as

$$\hat{S} = \hat{S}' + \hat{S}'' + \hat{S}''' \qquad (3)$$

where $\hat{S}' = \hat{S}_1 + \hat{S}_6$, $\hat{S}'' = \hat{S}_2 + \hat{S}_4$, and $\hat{S}''' = \hat{S}_3 + \hat{S}_5$. The general approach is to expand $\hat{S}^2$ and then reexpress $\hat{S}^2$ in terms of the Hamiltonian operator:

$$\hat{S}^2 = \hat{S}'^2 + \hat{S}''^2 + \hat{S}'''^2 + 2\hat{S}'\cdot\hat{S}'' + 2\hat{S}'\cdot\hat{S}''' + 2\hat{S}''\cdot\hat{S}''' \qquad (4)$$

$$\hat{S}^2 = \hat{S}'^2 + \hat{S}''^2 + \hat{S}'''^2 - (\hat{H}/J) \qquad (5)$$

Thus, the Hamiltonian operator can be expressed in terms of the total spin operator and the vector-coupling operators:

$$\hat{H} = -J[\hat{S}^2 - \hat{S}'^2 - \hat{S}''^2 - \hat{S}'''^2] \qquad (6)$$

For the cluster of six Cu(II) ions, there are five states with $S = 0$, nine states with $S = 1$, five states with $S = 2$, and one state with $S = 3$. The energies of these 20 states can be obtained from eq 6 and are

$$E(S = 3) = -6J$$

$$E(S = 2) = 0; 0; -2J; -2J; -2J$$

$$E(S = 1) = 4J; 4J; 4J; 2J; 2J; 0; 2J; 0; 0$$

$$E(S = 0) = 6J; 4J; 4J; 4J; 0 \qquad (7)$$

The Van Vleck equation for the magnetic susceptibility of the cluster can be written as

$$\chi_M = \frac{Ng^2\beta^2}{3k(T-\theta)}\frac{\sum_n S(S+1)(2S+1)\exp(-E_n^\circ/kT)}{\sum_n (2S+1)\exp(-E_n^\circ/kT)} + N\alpha \qquad (8)$$

where the summation runs over the cluster states with spin S, $N\alpha$ represents the second-order Zeeman terms, and the θ parameter has been added to account for intercluster interactions. Inserting the energies, E_n°, from eq 7 into eq 8 gives

$$\chi_M = \frac{2Ng^2\beta^2}{k(T-\theta)}\left[\left(14\exp\left(\frac{6J}{kT}\right) + 3\exp\left(\frac{-4J}{kT}\right) + 15\exp\left(\frac{2J}{kT}\right) + 3\exp\left(\frac{-2J}{kT}\right) + 13\right)\Big/\left(7\exp\left(\frac{6J}{kT}\right) + 12\exp\left(\frac{-4J}{kT}\right) + \exp\left(\frac{-6J}{kT}\right) + 15\exp\left(\frac{2J}{kT}\right) + 9\exp\left(\frac{-2J}{kT}\right) + 20\right)\right] + N\alpha \qquad (9)$$

Results of Magnetic Measurements. Three independent variable-temperature magnetic susceptibility data sets[16] were collected for a sample of **1**. The first two sets were run with a particular calibrated GaAs diode. To check the temperature calibration, we collected a complete data set for a $CuSO_4\cdot 5H_2O$ sample from 270 to 4.2 K in conjunction with the second running of the compound. The third data set was collected with a different calibrated GaAs diode and again a complete $CuSO_4\cdot 5H_2O$ magnetic susceptibility curve was run. Least-squares fitting of the three data sets to eq 9 gave J values of +4.9, +5.0, and +5.2 cm^{-1} with corresponding θ values of −2.5, −2.8, and −3.0 K. The g value was fixed at 2.066 which was obtained from the ~300 K Q-band EPR spectrum (vide infra). The temperature-independent paramagnetism ($N\alpha$) was estimated at 360×10^{-6} cgsu for the six Cu(II) ions in the complex. The function minimized was $\sum_{i=1}^{NP}\{[\chi_M(\text{calcd})_i - \chi_M(\text{obsd})]^2 T_i^2\}$ where NP is the number of experimental data points; the temperature weighting scheme prohibited overemphasis of the low-temperature data. The molar susceptibility for the entire compound and the effective magnetic moment (μ_{eff}) per Cu(II) ion are plotted as a function of temperature

(21) Colman, P. M.; Freeman, H. C.; Guss, J. M.; Murata, M.; Norris, V. A.; Ramshaw, J. A. M.; Venkatappa, M. P. *Nature (London)* **1978**, *272*, 319–24.
(22) Mastropaolo, D.; Thich, J. A.; Potenza, J. A.; Schugar, H. J. *J. Am. Chem. Soc.* **1977**, *99*, 424–9.
(23) McCandlish, L. E.; Bissell, E. C.; Coucouvanis, D.; Fackler, J. P.; Knox, K. *J. Am. Chem. Soc.* **1968**, *90*, 7357–9.
(24) Hollander, F. J.; Coucouvanis, D. *J. Am. Chem. Soc.* **1974**, *96*, 5646–8.
(25) Avdeef, A.; Fackler, J. P., Jr. *Inorg. Chem.* **1978**, *17*, 2182–7.
(26) Hatfield, W. E. In ref 10, 417–40.

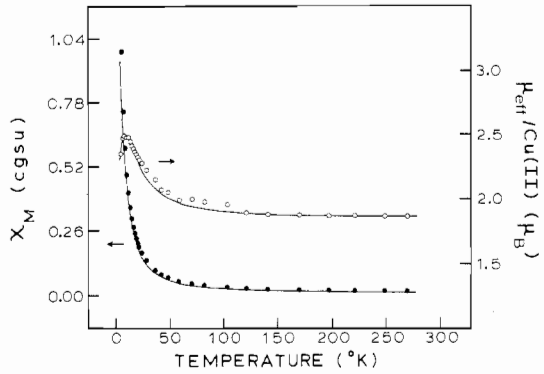

Figure 4. Experimental molar paramagnetic susceptibility (●) per cluster and effective magnetic moment (○) per Cu(II) ion vs. temperature for the cluster complex **1**. Solid lines represent the least-squares fit to the theoretical equation with $J = +4.9$ cm^{-1}, $g = 2.066$, and $\Theta = -2.5$ K.

in Figure 4 along with the least-squares fitting (as solid lines) to eq 9. For the data set displayed in Figure 4, μ_{eff} per Cu(II) varies from 1.86 μ_B at 270 K to 2.35 μ_B at 4.2 K, while for the other two data sets, these values range from 1.86 μ_B (270 K) and 1.79 μ_B (286 K) to 2.37 μ_B (4.2 K) and 2.37 μ_B (4.2 K).

EPR spectra of the mixed-valence copper cluster show a single derivative signal for powdered samples at either X- or Q-band frequencies regardless of sample temperature. The Q-band signal at ~300 K has a g value of 2.066 and a line width of 317 G measured as the half-width at half-height maximum (HWHM). Upon cooling of the sample to ~110 K, the g value changes slightly to 2.056 and the line width decreases to 291 G. The changes in the X-band EPR spectra are more pronounced. At temperatures of ~300, ~80, and 9 K, the single derivative has g values of 2.091, 2.098, and 2.069, respectively, while the HWHM decreases markedly with values of 338, 272, and 93 G.

EPR spectra were also recorded for the copper cluster run as a saturated 2:1 glycerol/water glass. The Q-band spectrum at 110 K shows a nearly isotropic signal at 2.065 with the indication of some poorly resolved hyperfine structure on the high-field side of the major derivative signal. The X-band glass spectrum also shows an isotropic signal with a g value of 2.091 at ~80 K and 2.063 at 9 K. The 9 K glass spectrum exhibited a "half-field" transition at 1620 G with an intensity of ~0.16 times that of the full-field transition.

Discussion of Magnetic Measurements. The magnetic susceptibility data support the structural result that 6 of the 14 copper ions are in the divalent state. Furthermore, as can be seen from the least-squares fit curve of the magnetic susceptibility to eq 9, a ferromagnetic exchange interaction is found for the mixed-valence copper cluster. Exchange coupling of six $S = {}^1/_2$ Cu(II) ions gives an $S' = 3$ ground state for a net ferromagnetic *intra*cluster interaction, and with only the ground state populated, the "spin-only" magnetic moment would be 2.83 μ_B per Cu(II) ion. Thus, the observed μ_{eff}/Cu(II) value of 2.35 μ_B at 4.2 K indicates that a substantial proportion of the molecules are in the $S' = 3$ ground state. It is important to note that a considerable number of SO_4^{2-} and H_2O molecules exist in the lattice which may serve to propagate the antiferromagnetic intercluster interaction. Such intercluster effects have often been noted,[27,28] particularly for complexes such as this one with a weak ferromagnetic intracluster exchange.

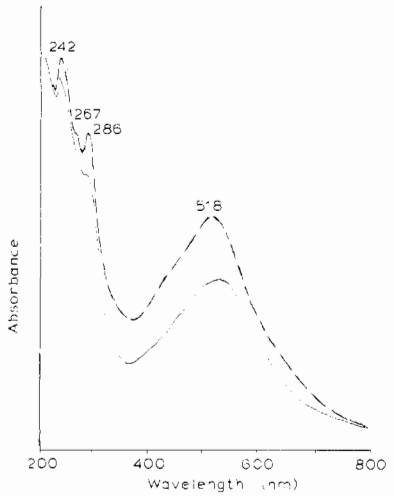

Figure 5. Electronic spectra at 273 K (—) and ca. 80 K (- - -) of **1** deposited as a polycrystalline film on a quartz disk.

Several examples of ferromagnetic exchange interactions in polynuclear copper(II) and nickel(II) complexes have been encountered.[26] In these ferromagnetic cluster complexes, the bridging ligands consist of single chlorine or oxygen atoms with M–X–M angles close to 90°. It is well-known that the orthogonality of p orbitals centered at the X-group results in these net ferromagnetic interactions. In the mixed-valence copper cluster, the observed ferromagnetic interaction probably is transmitted via a S–Cu(I)–S superexchange pathway. The diamagnetic Cu(I) ions show trigonal hybridization and it is the orthogonality of orbitals centered at the Cu(I) ion that leads to a net ferromagnetic interaction. An alternative superexchange pathway through a S–Cu(I)–Cl–Cu(I)–S moiety can be discounted due to the weak apical bonding of the central chloride ion to the Cu(I) ions.

The isotropic signals seen in the EPR spectra for the mixed-valence copper cluster can be understood by a consideration of the relative **g**-tensor alignment of the six Cu(II) ions and the effects of magnetic exchange. An examination of the cluster structure (Figure 1) shows that there are three different orientations of the approximately planar CuN_2S_2 units. Each Cu(II) site is related by a center of inversion to another and there are three of these pairs. With no exchange interaction present in the cluster, each Cu(II) ion would show one $g_{\|}$ and one $g_{\perp}$ signal. Since each Cu(II) environment is very similar, only one $g_{\|}$ and one $g_{\perp}$ signal would be seen for the cluster. As the exchange interaction increases in such a cluster, the frequency at which electrons exchange between Cu(II) ions increases. When the frequency of electron exchange exceeds the difference in $g_{\|}$ and $g_{\perp}$ values and when the Cu(II) ion environments are not *all* related by a center of inversion, the EPR signal becomes exchange averaged. Exchange averaging can result in a spectrum with only a single derivative signal, i.e., an "isotropic" signal.[29] This appears to be the situation in the present mixed-valence copper cluster. Additional support for this explanation comes from tabulated values[30] of monomeric square-planar Cu(II) complexes with N_2S_2 ligand coordination. The isotropic g values for these types of complexes fall in the range of 2.06–2.08, which compares very favorably with the g values (2.06–2.10) observed for our copper cluster. The isotropic g values observed for the glycerol–water glass mixture imply that the cluster remains intact in that

(27) Ginsberg, A. P.; Lines, M. E. *Inorg. Chem.* **1972**, *11*, 2289–90.
(28) McGregor, K. T.; Barnes, J. A.; Hatfield, W. E. *J. Am. Chem. Soc.* **1973**, *95*, 7993–8.
(29) Abragam, A.; Bleany, B. "Electron Paramagnetic Resonance of Transition Ions"; Clarendon Press: Oxford, England, 1970; pp 509–14.
(30) Goodman, B. A.; Raynor, J. B. *Adv. Inorg. Chem. Radiochem.* **1970**, *13*, 135. EPR parameters for monomeric CuN_2S_2 complexes are given in Table LIII, pp 316–7.

medium. Finally, we note that other workers have reported that the EPR spectrum of frozen aqueous $Na_5[Cu_{14}[SC(CH_3)_2CH(CO_2)NH_2]_{12}Cl]$ consists of a broad featureless absorption at $g \simeq 2$.[2] Such a result is in harmony with the fact that both complexes share a structurally similar $Cu_{14}S_{12}Cl$ unit.

Electronic Spectra of 1. The electronic spectra of polycrystalline **1** are presented in Figure 5. Aqueous **1** exhibits essentially identical, although somewhat less well-resolved spectral features, implying that the $Cu^I_8Cu^{II}_6[SC(CH_3)_2CH_2NH_2]_{12}Cl^{7+}$ unit persists as a solution as well as a lattice species. The observation that both **1** and the analogous copper–penicillamine cluster[31] elute from Sephadex G-25 as relatively sharp purple bands also implies that these clusters effectively are nonlabile. Extinction coefficients of the absorptions at 520, 282 (sh), 260 (sh), and 240 nm exhibited by aqueous **1** respectively are ~3400, ~5000, ~6000, and ~11 000 per Cu(II).

Before considering the electronic spectra further, it is worthwhile to review selected structural features of **1** and related complexes. The crystallographic and magnetochemical results above support the notion that distinct planar-coordinated Cu(II) ions and dominantly trigonal-coordinated Cu(I) ions are present in **1** and that metal–metal interactions within the $Cu^I_8[SC(CH_3)_2CH_2NH_2]_{12}Cl$ substructure are weak. Consequently, electronic–structural peculiarities are not expected of the cubic substructure unit. If such a unit could be isolated as a separate entity, it might be expected to be a typical copper(I)–mercaptide complex which is yellow due to tailing of S → Cu(I) charge-transfer absorptions centered in the UV region. The precursor complexes **2** and **3** and several fully characterized Cu(II)–mercaptide complexes studied by other workers are yellow materials.[32] Since the Cu(I) and Cu(II) ions are joined by bridging mercaptide ligands, the possibility of mixed-valence electronic absorption arises. Systems which exhibit broad prominent absorptions of this type have ligand donor sites which readily can accommodate the metal ion in both valence states of interest.[33] Mixed-valence Cu(I)/Cu(II) systems with both Cl^- and carboxylate bridging ligands have been characterized by other workers.[34] The substantial structural differences between the N_2S_2 and S_3 donor sets in **1** should serve to make the following process improbable:

$$Cu^{II}N_2S_2 + Cu^{I}S_3 \xrightarrow{h\nu} Cu^{I}N_2S_2 + Cu^{II}S_3$$

The cluster structure of **1** bears a certain resemblance to that reported for the trinuclear $Ni[Ni(NH_2CH_2CH_2S)_2]_2^{2+}$ complex.[35] The planar S_4 ligand set of the central Ni(II) ion is supplied by an appropriate arrangement of two planar and otherwise typical $Ni(NH_2CH_2CH_2S)_2$ units which are capable of independent existence. In a similar fashion, we may consider the Cu(II) ions in **1** to be ligated by sulfur donors of the $Cu^I_8S_{12}Cl^{5-}$ substructure along with its 12 primary amine "tails". Three chloride-free $Cu_8S_{12}^{4-}$ substructures[23,24] as well as the $Cu_8S_{12}Cl^{5-}$ substructures in **1** and the copper–penicillamine analogue[2] have been characterized crystallographically. Moreover, a $[Cd_8(SCH_2CH_2OH)_{12}I]^{3+}$ cluster exhibits the corresponding $Cd_8S_{12}I^{3+}$ substructure to which are attached 12 $-CH_2CH_2OH$ tails[36] that in principle are capable of binding external ions. These results are consistent with the view that the $Cu_8S_{12}Cl^{5-}$ substructure in **1** along with the 12 attached $-C(CH_3)_2CH_2NH_2$ tails may be considered as a ligand for Cu(II). When viewed this way, **1** is *not* a copper(II)–mercaptide complex but rather Cu(II) bound to a copper(I)–mercaptide cluster, and the usual redox instability of copper(II) mercaptides may be circumvented.

We now consider the strong electronic absorption (ϵ ~3400 per Cu(II)) exhibited by **1** at ~19 300 cm^{-1} (530 nm). Other workers[25] recently have reported MO calculations and electronic spectra of $(Pr_4N^+)_4Cu_8[S_2C{=}C(CN)_2]_6^{4-}$. Mull spectra of this salt revealed strong absorptions at 19 600 and 26 000 cm^{-1} which were blue shifted to 24 800 cm^{-1} (ϵ 2.3 × 10^4 per cluster) and 31 200 cm^{-1} (ϵ 1.8 × 10^4 per cluster) when the salt was dissolved in ethanol. The first symmetry-allowed absorption was predicted to be a S(3p) → Cu(4s,4p) charge-transfer transition and the intense absorption at ~20 000 cm^{-1} was assigned to this process.[25] In contrast, aqueous *and* polycrystalline **1** exhibit similar absorptions at ~19 300 cm^{-1}. Moreover, reference Cu(I) clusters of conventional aliphatic and aromatic mercaptides do not exhibit intense low-energy absorptions. Thus, the absorption bands cited above for the $Cu_8[S_2C{=}C(CN)_2]_6^{4-}$ cluster presumably arise because of the special electronic–structural nature of $S_2C{=}C(CN)_2^{2-}$, and the absorptions of **1** at ~19 300 cm^{-1} should have a different origin. In view of the markedly different Cu(I) and Cu(II) coordination geometries in **1**, the origin of this band is not likely to be an intervalence transition. As noted above, such a spectroscopic process for **1** should not have substantial intensity. Also, the appearance of the absorption at ~19 300 cm^{-1} differs from the intervalence absorption exhibited by a Cu(I)/Cu(II) acetate system.[34] Finally, the intensity of the absorption at 19 300 cm^{-1} is too large to be fully accounted for by a ligand field transition of a planar $Cu^{II}N_2S_2$ chromophore. Although distorted five-coordinate Cu(II) complexes may exhibit fairly intense (ϵ ~1000) LF absorptions,[20] tetragonal or planar Cu(II) chromophores exhibit weaker (ϵ ~100–300) absorptions. Since a *trans*-$Cu^{II}N_2(S\text{-thioether})_2$ chromophore exhibits a LF absorption at ~550 nm,[37] presumably the LF absorption of the $Cu^{(II)}N_2S_2$ chromophore in **1** is contained within the envelope of the band centered at 19 300 cm^{-1}. Assuming that the Cu(II) ions in **1** are ligated by the $Cu_8S_{12}Cl^{5-}$ substructure, the Cu(II)–S bonds are expected to have a character intermediate between Cu(II)–thioether and Cu(II)–mercaptide. The σ(*S*-thioether) → Cu(II) charge-transfer absorption for the above *trans*-$Cu^{II}N_2(S\text{-thioether})_2$ chromophore has been observed at ~390 nm.[37] The corresponding absorption for the *cis*-$Cu^{II}N_2S_2$ chromophore may be expected to be red-shifted somewhat. Therefore, we think that the absorption of **1** at ~19 300 cm^{-1} reasonably may be assigned to σ(S) → Cu(II) charge transfer. Mercaptide complexes of Cu(II) and Co(II) exhibit intense σ(S) → M(II) charge transfer as well as one or two weaker, red-shifted absorptions which have been assigned to π(S) → M(II) charge transfer.[20,22,38–40] Complex **1** does not exhibit a weaker red-shifted counterpart of the band at 19 300 cm^{-1} which would correspond to π(S) → Cu(II) charge transfer. The absence of such a band may be expected because the relevant electron pairs of S both are localized within strong Cu(I)–S bonds and have poor availability for π bonding with the Cu(II) ions. Finally, the band system in the 242–286-nm region presumably includes the expected S → Cu(4s,4p) charge-transfer absorption along with the expected σ(N) →

(31) Wright, J. R.; Frieden, E. *Bioinorg. Chem.* **1975**, *4*, 163–75.
(32) Dance, I. G. *Aust. J. Chem.* **1978**, *31*, 2195–206 and references cited therein.
(33) Robin, M. B.; Day, P. *Adv. Inorg. Chem. Radiochem.* **1967**, *10*, 247–422.
(34) Sigwart, C.; Hemmerich, P.; Spence, J. T. *Inorg. Chem.* **1968**, *7*, 2545–8.
(35) Wei, C. H.; Dahl, L. F. *Inorg. Chem.* **1970**, *9*, 1878–87.
(36) Bürgi, H. B. *Helv. Chim. Acta* **1976**, *59*, 2558–65.
(37) Miskowski, V. M.; Thich, J. A.; Solomon, R.; Schugar, H. J. *J. Am. Chem. Soc.* **1976**, *98*, 8344–50.
(38) Solomon, E. I.; Hare, J. W.; Gray, H. B. *Proc. Natl. Acad. Sci. U.S.A.* **1976**, *73*, 1389–93.
(39) McMillin, D. R.; Rosenberg, R. C.; Gray, H. B., *Proc. Natl. Acad. Sci. U.S.A.* **1974**, *71*, 4760–2.
(40) Tennent, D. L.; McMillin, D. R. *J. Am. Chem. Soc.* **1979**, *101*, 2307–11.

Cu(II) charge-transfer absorption. This latter absorption is exhibited by a variety of tetragonal Cu(II)–amine complexes in the 240–270-nm spectral region.[37]

Acknowledgment. Research at Rutgers was supported by the National Institutes of Health (Grant AM-16412 to H.J.S.), by the Research Corp. (Grant to H.J.S.), and by generous grants of computing time from the Center for Computer and Information Services, Rutgers University. Research at Illinois was supported by the National Institutes of Health (Grant HL-13652 to D.N.H.).

Registry No. **1**, 72214-16-5; **2**, 72244-66-7; **3**, 72244-67-8; $Cu(CH_3CN)_4ClO_4$, 14057-91-1.

Supplementary Material Available: Listings of structure factor amplitudes and experimental and calculated magnetic susceptibility data for **1** (28 pages). Ordering information is given on any current masthead page.

Notes

Contribution from the Department of Chemistry, University of Stellenbosch, Stellenbosch 7600, Republic of South Africa

Potentiometric Investigation of Molybdenum(VI) Equilibria at 25 °C in 1 M NaCl Medium

J. J. Cruywagen

Received June 19, 1979

The well-established method of equilibrium analysis by potentiometric titration in a medium of constant and high ionic strength has been used by several authors to obtain information about the various mono- and polynuclear species which may exist in acidified molybdate solutions.[1-5] In the pH range for which the degree of protonation is less than 1.5, results of these studies were interpreted mainly in terms of hexa-, hepta- and octamolybdates,[1-5] in addition to the monomeric species $HMoO_4^-$ and $Mo(OH)_6$.[6] Sasaki and Sillén[4] found a series of heptamolybdates to predominate in 3.0 M $NaClO_4$ medium, viz., (8, 7), (9, 7), (10, 7), and (11, 7), the numbers referring to the values of p and q in the general formula $H_pMo_7O_{24}^{(p-2q)}$. From the results of an investigation in 1.0 M NaCl, Aveston et al.[2] also proposed a series of heptamers but considered the octameric ion (12, 8) more likely than the (11, 7) species. These authors based their findings on other experimental methods as well. Schwing[3] concluded that the species (8, 6), (8, 7), and probably also (9, 6) exist in 3.0 M NaCl medium.

The potentiometric data from the above-mentioned studies were subsequently treated by Sillén[7] with his "species selector" program LETAGROP. Although the reaction model giving the best fit in each case included the polynuclear ions (8, 7), (9, 7), (10, 7), and (11, 7), no single model could satisfy all three sets of data with respect to the selection criteria adopted in the program.

More recently Baldwin and Wiese[5] conducted a potentiometric investigation in 1 M $Mg(ClO_4)_2$ medium, and again using the program LETAGROP for the treatment of their data, they found as major polynuclear components the ions (8, 6) and (9, 8).

Although medium effects may account for some of the inconsistencies, it appears as if potentiometric data as such do not lead to a complete description of all the simultaneous condensation and protonation equilibria of molybdenum(VI) in acid solution. However, the interpretation of results obtained by other important experimental methods, e.g., enthalpimetric and kinetic methods, depends heavily on values of equilibrium constants determined by potentiometry. For instance the results of an extensive kinetic study by temperature jump,[8] which pointed to the (12, 8) species rather than the (11, 7), were interpreted by using the equilibrium constants reported by Aveston et al.;[2] the values of $\beta_{9,7}$ and $\beta_{10,7}$ had, however, to be adjusted by 1 log unit to give the best fit between observed and calculated relaxation times. This discrepancy and the need for reliable equilibrium constants for use in the treatment of results of an extensive calorimetric investigation of molybdenum(VI) equilibria in 1 M NaCl medium, currently being conducted in our laboratory, necessitated the present investigation.

Experimental Section

Reagents and Materials. All reagents were of analytical grade (Merck p.a.) and solutions were prepared with deionized distilled water. Sodium chloride solution was prepared from recrystallized NaCl and standardized by drying samples to constant weight at 130 °C. Prior to recrystallization, a saturated solution of salt was allowed to stand for about a week during which time some impurities precipitated. Sodium molybdate, $Na_2MoO_4 \cdot 2H_2O$, was purified and recrystallized as described by Sasaki and Sillén.[4] The stock solution, standardized gravimetrically by precipitation of molybdate as $PbMoO_4$,[9] was kept in a polythene bottle. Hydrochloric acid was standardized indirectly against potassium hydrogen phthalate by titration with sodium hydroxide.

Potentiometric Measurements. The experiments were carried out as titrations at 25.0 ± 0.1 °C in a waterbath starting with 100 mL sodium molybdate and adding hydrochloric acid from a 10 mL buret. Sodium chloride was used to maintain the chloride concentration of the solutions at 1.0 M. A stream of nitrogen, free from carbon dioxide, was presaturated with 1.0 M NaCl and used for stirring the solution.

The hydrogen ion concentration, h, of the solution was determined by measuring the emf accurate to ±0.1 mV with a Beckman Research pH meter employing Beckman glass (39000) and Beckman calomel (39071) electrodes. The electrode system was standardized by a similar titration of 1 M NaCl with hydrochloric acid and the value of $E°$ determined from the measured emf values (in mV) by using eq 1.

$$E = E° + 59.15 \log h \quad (1)$$

A value for $E°$ was determined before each titration of molybdate with acid and checked afterwards by a single emf measurement of the same solution used to determine $E°$. The titration data were considered acceptable only if the difference between the $E°$ values was ≤0.3 mV. Titrations were carried out at $-\log h$ values ranging from 6.5 to 2 at the following (initial) molybdenum(VI) concentrations: 0.0005, 0.001 (two), 0.002, 0.005, 0.01, 0.05, and 0.10 M. Of these, 324 experimental points corresponding to a degree of protonation of ≤1.5 were used in the computation of the stability constants.

Results and Discussion

Treatment of Data. The equilibria for the various possible condensation and protonation reactions can be represented by the general equation

(1) Y. Sasaki and L. G. Sillén, *Acta Chem. Scand.*, **18**, 1014 (1964).
(2) J. Aveston, E. W. Anacker, and J. S. Johnson, *Inorg. Chem.*, **3**, 735 (1964).
(3) J. P. Schwing, *J. Chim. Phys. Phys.-Chim. Biol.*, **61**, 508 (1964).
(4) Y. Sasaki and L. G. Sillén, *Ark. Kemi*, **29**, 253 (1968).
(5) W. G. Baldwin and G. Wiese, *Ark. Kemi*, **31**, 419 (1969).
(6) J. J. Cruywagen and E. F. C. H. Rohwer, *Inorg. Chem.*, **14**, 3136 (1975).
(7) L. G. Sillén, *Pure Appl. Chem.*, **17**, 55 (1968).
(8) D. S. Honig and K. Kustin, *Inorg. Chem.*, **11**, 65 (1972).
(9) A. I. Vogel, "A Textbook of Quantitative Inorganic Analysis", 3rd ed., Longmans, Green and Co., New York, 1961, p 506.

0020-1669/80/1319-0552$01.00/0